

Gravitational Waves from Density Perturbations in an Early Matter Domination Era

Ioannis Dalianis ^{ab} and Chris Kouvaris ^a

^a *Physics Division, National Technical University of Athens,
15780 Zografou Campus, Athens, Greece*

^b *Department of Physics, University of Athens,
University Campus, Zographou 15784, Greece*

E-mail : dalianis@mail.ntua.gr, kouvaris@mail.ntua.gr

Abstract

We calculate the gravitational wave background produced from density perturbations in an early matter domination era where primordial black holes form. The formation of black holes requires perturbations out of the linear regime. Space with such perturbations reach a maximum expansion before it collapses asymmetrically forming a Zel'dovich pancake which depending on the parameters can either lead to a black hole or a virialized halo. In both cases and due to the asymmetry of the collapsing matter, a quadrupole moment generates gravitational waves which leave an imprint in the form of a stochastic background that can be detectable by near future gravitational interferometers.

1 Introduction

With the advent of gravitational wave (GW) detection from mergers of black holes [1], a new era of exploration has begun that could accelerate our progress in understanding black hole physics and the conditions of the early universe. Apart from pure astrophysical processes like the merger of two black holes or neutron stars, gravitational interferometers could also probe the early universe for example by observing mergers of primordial black holes or by observing a stochastic gravitational wave background produced from process much earlier than the formation of the first stars. The LIGO collaboration has already produced upper limits in such stochastic backgrounds [2]. This will be further extended in the near and not so near future, by a network of operating and designed gravitational wave detectors that will probe a vast range of different frequency bands. Pulsar time array (PTA) GW experiments [3] have a sensitivity at the nHz frequency band, space-based designed interferometers like LISA [4], Taiji [5], Tianqin [6], Decigo [7, 8] are mostly sensitive to milli- and deci-Hz frequency bands and the LIGO/Virgo and Einstein telescope [9] ground based interferometers are sensitive to larger frequencies.

Several physical sources that generate GWs in the early universe have been proposed so far [10–14]. Among them there is an unambiguous source: the primordial density scalar perturbations that source tensor modes at non-linear order perturbation theory [15–20], the so-called induced or secondary gravitational waves. Density perturbations in the non-linear regime induce tensors with amplitudes proportional to the square of the density perturbations. The induced tensors are suppressed by the small $\delta\rho/\rho$ value at the CMB scales [21], but might be sizable if the primordial curvature perturbations are enhanced at small scales. A potential detection of the relic GW stochastic background might be a direct probe of the very early cosmic history, which is unknown for $t \lesssim 1\text{s}$ [22].

The features of the induced GWs are well understood and described if the associated gravitational potential decays with time. This is the case for the radiation domination era [23–26]; results also exist for a background with non-thermal, but non-zero, pressure [27–29]. On the other hand, the gravitational potential during a matter dominated universe remains constant and the density perturbations grow. Ref. [30] pointed out the limitations of the perturbative analysis due to the presence of a non-linear scale. Inside the perturbative regime, Ref. [31, 32] performed a thorough investigation where the role and contribution of the subhorizon perturbations has been stressed. However, the non-linear scale restricts the applicability of the existing formalism only on a short period before the reheating of the universe and the transition into the radiation era. In addition, the induced tensors are generated from quadratic combinations of first order scalars and during matter era are continuously sourced and thus do not propagate freely; this fact raises an issue of gauge dependence, discussed in [33–40].

In this work, motivated by the above theoretical and analytical limitations we choose to tackle the problem of the computation of the GW signal during an early matter domination era (eMD) following an alternative analytic yet nonlinear approach. Studying nonlinear gravitation instability is notoriously difficult even within the Newtonian context. However, the pioneering work of Zel’dovich [41] have shown that there can be an approximation valid well inside the nonlinear regime (although eventually breaks down too) [42]. The Zel’dovich approximation describes the nonlinear evolution of pressureless density perturbations which deviate from the sphere. As the system evolves, an initial deviation from the spherical shape becomes more pronounced as times goes on, leading to flattened structures the so-called Zel’dovich pancakes. This increasingly asymmetric evolution of the collapsing perturbation creates substantial quadrupole moment which in turn creates GWs. The approximation breaks at some point and the eventual fate of the collapsing perturbation is dictated by the final degree of asymmetry of the pancake. If the final configuration (i.e. the pancake) satisfies the hoop conjecture [43, 44], a black hole is formed out of this collapsing chunk of matter. If the hoop conjecture is not satisfied, the pancake will go through a phase of shell crossing and oscillation due to its asymmetry redistributing the energy among the different particles leading via violent relaxation to a state of a virialized halo [45]. In this paper we focus on the first part of the process, i.e. the nonlinear collapse of the perturbation within the Zel’dovich approximation and we will not address here the background that could potentially exist due to the violent relaxation of the Zel’dovich pancakes. Since our approach is based on the aforementioned nonlinear treatment of the perturbation, we circumvent the limitations of the perturbation theory which is strictly valid in the linear regime.

We note that the GW emission during an eMD era and in the non-linear regime has been discussed in the past in Ref. [46], and later in Ref. [47]. The early work [46] gave a description of the non-linear phases until the moment of reheating and an order of magnitude estimation for the total GW signal. Here, aiming at a refined result, we derive a new expression for the spectrum of the GW signal produced during the collapsing phase following the Zel’dovich approximation.

Our method provides semi-analytic results that complements the GR perturbative approach in the non-linear regime and lightens the underlying physical processes helping thus to identify the physical quantities and pin down the signatures of the GWs. In addition to the GW spectra we examine the abundance and distribution of the associated primordial black holes (PBHs). We examine scenarios that predict a sizable amount of both PBHs and GW background, and scenarios that predict a significant amount of GWs with the PBH counterpart being either negligibly small or promptly evaporating and we manifest the connection between the PBH mass and the GW counterpart. Our results can be used to test already existing and viable inflationary models in which PBHs are produced in an eMD phase [48–50].

It is worth stating that an eMD phase of the universe is well motivated in several beyond Standard Model scenarios. Such a phase happens before the universe is dominated by radiation and it can practically last almost up $t \simeq 1$ sec which is the start of Big Bang Nucleosynthesis (BBN).

The paper is organized as follows. In section II we describe the evolution of a density perturbation characterized by a small deviation from sphericity. In section III we derive the general formula for the spectral energy density of the GWs. In section IV we estimate the GW signal and amplitude following analytic steps and approximations. In section V we connect the GW signal with the associated PBH abundance. We conclude in section VI.

2 Evolution and collapse of the overdensities in eMD

As we mentioned in the introduction we will not use second order perturbation theory in order to find the GW induced by the overdensities, but we will estimate the quadrupole moment of pressureless collapsing matter within the Zel'dovich approximation. Here we will closely follow the detailed analysis of [51]. Within the Zel'dovich approximation, the coordinate of a particle is written as

$$r_i = a(t)q_i + b(t)p_i(q_i), \quad (1)$$

where $a(t)$ is the usual scale factor encoding the expansion of the Universe, q_i is the comoving coordinate, $b(t)$ is a growing mode encapsulating the gravitational instability in a pressureless eMD universe and p_i are deviation vectors that depend on the initial perturbation. In order to study the motion of a group of particles around q_i , a deformation (strain) tensor D_{ik} is needed defined as

$$D_{ik} = \frac{\partial r_i}{\partial q_k} = a(t)\delta_{ik} + b(t)\frac{\partial p_i}{\partial q_k} \quad (2)$$

$$= \text{diag}(a - \alpha b, a - \beta b, a - \gamma b), \quad (3)$$

where we have chosen our comoving coordinate system so that the matrix $\partial p_i/\partial q_k$ is diagonal,

$$\frac{\partial p_i}{\partial q_k} = -\text{diag}(\alpha, \beta, \gamma). \quad (4)$$

A perturbation with size q and wavenumber $k = q^{-1}$ enters the horizon at t_q satisfying

$$a(t_q)q = H^{-1}(t_q). \quad (5)$$

We assume initially small deviations from sphericity, $\alpha b(t_q)/a(t_q) \ll 1$, $\beta b(t_q)/a(t_q) \ll 1$, $\gamma b(t_q)/a(t_q) \ll 1$ so that we can say that at t_q nearly the whole ellipsoid is inside the Hubble sphere, $r_i(t_q) \approx a(t_q)q$, where \vec{r} is the position of the ellipsoid boundary. The mass contained in the overdensity is conserved i.e.,

$$M = \int \rho a^3 d^3 r = \bar{\rho} a^3 \int d^3 q, \quad (6)$$

leading to the following relation between densities

$$\rho(a - \alpha b)(a - \beta b)(a - \gamma b) = \bar{\rho} a^3. \quad (7)$$

The energy contrast after truncating terms beyond the linear order reads

$$\delta_L \equiv \left(\frac{\rho - \bar{\rho}}{\bar{\rho}} \right)_L = (\alpha + \beta + \gamma) \frac{b}{a} \quad (8)$$

where $b(t)\alpha \ll a(t)$, $b(t)\beta \ll a(t)$, $b(t)\gamma \ll a(t)$. At the moment of horizon entry, the density contrast field is

$$\delta_L(t_q) = (\alpha + \beta + \gamma) \frac{b(t_q)}{a(t_q)} \ll 1. \quad (9)$$

Shrinking takes place for positive $\delta_L > 0$. When $\delta_L \rightarrow 1$ the expression (8) stops being valid. It is known [52] that during matter domination the density perturbation in the linear regime grows as the scale factor, $\delta \propto a$. Hence,

$$b \propto a^2, \quad (10)$$

signifying that the growing mode $b(t)$ of the deformation tensor describing the collapse, changes much more rapidly than the Hubble flow factor $a(t)$. The perturbation will collapse at least along one of the three axes and here we assume that

$$\alpha > 0, \quad -\infty < \gamma \leq \beta \leq \alpha < \infty \quad \text{and} \quad \alpha + \beta + \gamma > 0. \quad (11)$$

From Eqs. (5) and (6) one can relate the horizon entry time t_q with the mass contained

$$t_q = \frac{4GM}{3}. \quad (12)$$

We define four important moments: The horizon entry time t_q , the maximum expansion time t_{\max} , the collapse time t_{col} and the (potential) BH formation time t_{BH} . At the moment of maximum expansion, that we labeled t_{\max} , the mass is about to shrink. By definition it is $\dot{r}_1(t_{\max}) = 0$ and one finds $\dot{a}(t_{\max}) = \alpha \dot{b}(t_{\max})$. This implies $\dot{b}/\dot{a} = 1/\alpha$ at the maximum expansion and

$$r_1(t_{\max}) = a(t_{\max})q_1 - \alpha b(t_{\max})q_1 = \frac{1}{2}a(t_{\max})q_1, \quad (13)$$

which means that at maximum expansion the 1st-axis, r_1 , has half of the size the primordial perturbation would have due to the Hubble flow only. Since $b \propto a^2$, $\dot{b} \propto 2a\dot{a}$ one finds

$$\frac{b(t_{\max})}{a(t_{\max})} = \frac{1}{2\alpha}. \quad (14)$$

Since we know the ratio of $b(t)/a(t)$ at both t_q and t_{\max} from Eqs. (9) and (14), we can write

$$\frac{a(t_{\max})}{a(t_q)} = \frac{\alpha + \beta + \gamma}{2\alpha\delta_L(t_q)}. \quad (15)$$

Taking into account that $a(t) \propto t^{2/3}$ during matter domination leads us to

$$t_{\max} = \left(\frac{\alpha + \beta + \gamma}{2\alpha\delta_L(t_q)} \right)^{3/2} t_q. \quad (16)$$

2.1 Pancake collapse of the overdensity

Collapse takes place at the time t_{col} where $r_1(t_{\text{col}}) = 0$. It is $a(t_{\text{col}})q_1 = \alpha b(t_{\text{col}})q_1$ and the ratio of the scale factor and the linearly growing mode $b(t)$,

$$\frac{b(t_{\text{col}})}{a(t_{\text{col}})} = \frac{1}{\alpha}. \quad (17)$$

This is a pancake collapse because the mass becomes a two-dimensional ellipse with the semi-minor and semi-major axes given by $r_2(t_{\text{col}})$ and $r_3(t_{\text{col}})$. The relation $b \propto a^2$ implies then

$$\frac{b(t_{\text{col}})}{b(t_{\max})} = \left(\frac{a(t_{\text{col}})}{a(t_{\max})} \right)^2, \quad (18)$$

and from Eq. (17) one finds $a(t_{\text{col}}) = 2a(t_{\max})$. The scale factor changes with the cosmic time as $a \propto t^{2/3}$, hence

$$t_{\text{col}} = 2^{3/2}t_{\max} \simeq 2.8t_{\max}. \quad (19)$$

The semi-minor and semi-major axes of the overdensity at the time of collapse depend essentially on the values of the deformation parameters α, β and γ ,

$$r_2(t_{\text{col}}) = 4r_1(t_{\max}) \left(1 - \frac{\beta}{\alpha} \right) = 2a(t_{\max})q \left(1 - \frac{\beta}{\alpha} \right), \quad (20)$$

$$r_3(t_{\text{col}}) = 4 r_1(t_{\text{max}}) \left(1 - \frac{\gamma}{\alpha}\right) = 2 a(t_{\text{max}}) q \left(1 - \frac{\gamma}{\alpha}\right). \quad (21)$$

We see that for $\beta \sim 0$ and $\gamma \sim 0$ the non-collapsed other two dimensions might have grown nearly freely due to the background expansion having size $a(t_{\text{col}})q$. Also for β and γ not much smaller than the α , i.e. $\alpha \sim \beta \sim \gamma$ we have a spherical collapse and a black hole might form.

Let us mention that, except for the time of maximum expansion for the $r_1(t)$ axis, one can find the time of maximum volume. For the special case $\beta \sim \gamma \sim 0$ the equation $\dot{V}_{\text{ellip}}(t_{\text{maxV}}) = 0$ implies that $b/a = 3/(4\alpha)$ and one finds $t_{\text{maxV}} \sim (3/2)^{3/2} t_{\text{max}}$. The moment t_{maxV} is the moment of minimum density value of the perturbation and signifies a turnover. It is $\dot{\rho}_{\text{ellip}}(t_{\text{maxV}}) = 0$ and afterward the density increases. We see that at least until that time the Zel'dovich approximation is reliable and any error at the estimation of t_{col} should be of order $\mathcal{O}(1)$.

The t_{col} can be calculated for particular values of the parameters $\delta_L(t_q)$, t_q and α, β, γ , i.e. $t_{\text{col}} = t_{\text{col}}(\alpha, \beta, \gamma, \delta_L, t_q)$. The $\delta_L(t_q)$ is specified by the amplitude of the power spectrum peak; t_q is specified by the position of the curvature power spectrum peak; α, β, γ are specified by the Doroshkevich probability function that we introduce right below.

2.2 Probability distribution of parameters of the deformation tensor

The Doroshkevich probability distribution of α , β and γ encapsulates and quantifies the finite probability that the considered overdensity deviates from sphericity. It reads [53],

$$\begin{aligned} \mathcal{F}_D(\alpha, \beta, \gamma, \sigma_3) d\alpha d\beta d\gamma = & - \frac{27}{8\sqrt{5}\pi\sigma_3^6} \times \exp \left[- \frac{3}{5\sigma_3^2} \left((\alpha^2 + \beta^2 + \gamma^2) - \frac{1}{2}(\alpha\beta + \beta\gamma + \gamma\alpha) \right) \right] \\ & \times (\alpha - \beta)(\beta - \gamma)(\gamma - \alpha) d\alpha d\beta d\gamma, \end{aligned} \quad (22)$$

for $\alpha \geq \beta \geq \gamma$ and is normalized to one,

$$\int_{-\infty}^{\infty} d\alpha \int_{-\infty}^{\alpha} d\beta \int_{-\infty}^{\beta} d\gamma \mathcal{F}_D(\alpha, \beta, \gamma, \sigma_3) = 1 \quad (23)$$

The σ is the standard deviation of $\delta_L(t_q)$, given by the expectation value of the density perturbation at the moment of entry

$$\sigma^2 = \langle \delta_L^2(t_q) \rangle = \langle (\alpha + \beta + \gamma)^2 \rangle \left(\frac{b}{a} \right)^2 (t_q) = 5\sigma_3^2, \quad (24)$$

after fixing the normalization of β as $b(t)/a(t) = a(t)/a(t_i)$. The probability that the sum of the difference between α, β and γ takes a value much larger than $\sigma_3 = \sigma/\sqrt{5}$ is exponentially suppressed. The most probable values are

$$\alpha = \mathcal{O}(\sigma_3), \quad \beta = \mathcal{O}(\sigma_3), \quad \gamma = \mathcal{O}(\sigma_3), \quad (25)$$

as one can see from Fig. 1; thus there is a σ_3 deviation from sphericity. Note that the exact spherical configuration $\alpha = \beta = \gamma$ has zero Doroshkevich probability density.

In our case we add to the hierarchy (11) for the α, β and γ values the extra constraint that the time of maximum expansion t_{max} is larger than the time of entry t_q ,

$$\alpha + \beta + \gamma > 2\alpha\sigma \quad (26)$$

Therefore we constrain the integration region of the Doroshkevich probability density in the subspace \mathcal{S} ,

$$\begin{aligned} 0 < \alpha < \infty \\ -\frac{\alpha}{2}(1 - 2\sigma) < \beta < \alpha \\ -\beta - \alpha(1 - 2\sigma) < \gamma < \beta \end{aligned} \quad (27)$$

Fig. 1 shows the behavior of the distribution in different cases, given the hierarchy (27). We mention that the triple integral (22) can be calculated analytically over the γ direction and a two dimensional distribution is obtained.

The standard deviation of the density perturbation theory is related to the power spectrum of the density contrast $\sigma = \sqrt{\mathcal{P}_\delta}$. The density perturbation in the linear regime in the Newtonian gravity coincides with that in the relativistic perturbation theory in comoving slicing both at subhorizon and superhorizon scales in the matter dominated phase [51, 54, 55]. At horizon crossing the variance σ is related as $\sqrt{\mathcal{P}_\delta} = (2/5)\sqrt{\mathcal{P}_\mathcal{R}}$ where $\mathcal{P}_\mathcal{R}$ is the commonly used, e.g. in inflation model building, power spectrum of the curvature perturbation defined on comoving hypersurfaces.

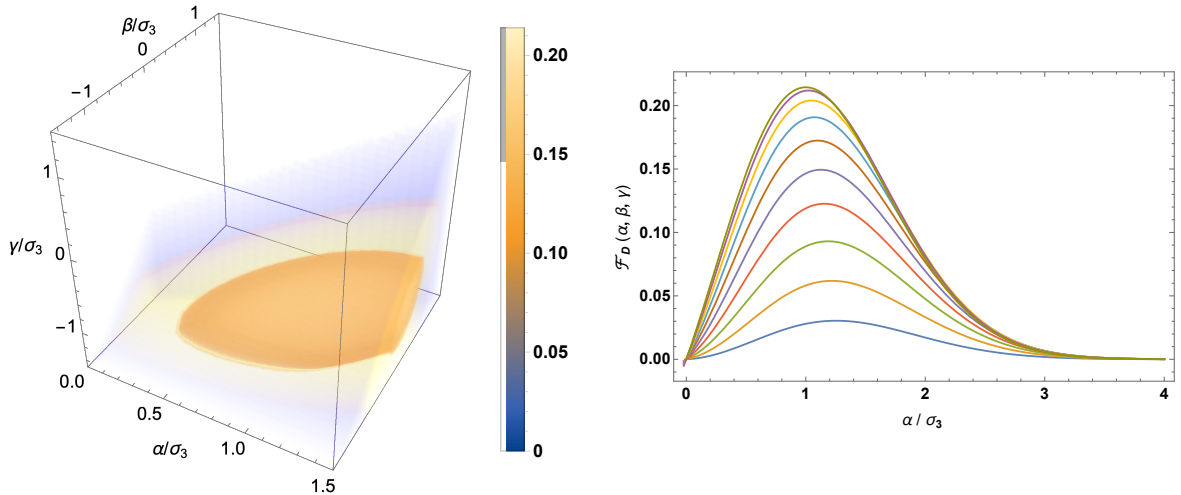


Figure 1: *Left panel:* Density plot for the Doroshkevich probability density \mathcal{F}_D for α, β, γ normalized by the variance σ_3 . *Right Panel:* One dimensional section of the Doroshkevich probability density with respect to the parameter α/σ_3 for ten different γ/σ_3 values from $\gamma = -0.1\sigma_3$ (lower curve) to $\gamma = -\sigma_3$ (upper curve) and $\beta/\sigma_3 = 0$.

3 Derivation of the energy density of GWs

The GW emission is described by a multipole expansion of the perturbation $h_{\mu\nu}$ to a background spacetime $g_{\mu\nu}$. To lowest order $h_{ij}(t, d) \propto \dot{Q}_{ij}(t - d/c)/d$, where Q_{ij} is the mass quadrupole moment and d the distance from the source. In terms of the moment of inertia the quadrupole moment is written as

$$Q_{ij} = -I_{ij}(t) + \frac{1}{3}\delta_{ij}\text{Tr}I(t), \quad (28)$$

where I_{ij} is the moment of inertia tensor¹. By choosing the principal axes frame, the moment of inertia tensor is

$$I_{ij} = \frac{1}{5}M \begin{pmatrix} r_2^2 + r_3^2 & 0 & 0 \\ 0 & r_1^2 + r_3^2 & 0 \\ 0 & 0 & r_1^2 + r_2^2 \end{pmatrix}, \quad (29)$$

where M is the constant mass enclosed by the ellipsoid.

Using Eq. (1) and the fact that $b(t) \propto a^2(t)$, we can write the coordinates as a function of time as

$$r_1(t) = \frac{3}{2}t_q^{1/3}t^{2/3} \left(1 - \frac{1}{2} \left(\frac{t}{t_{\max}} \right)^{2/3} \right),$$

¹It is defined as

$$I_{ij} = \int d^3x \rho(\vec{x}) (\delta_{ij}|\vec{x}|^2 - x_i x_j).$$

$$r_2(t) = \frac{3}{2} t_q^{1/3} t^{2/3} \left(1 - \frac{\beta}{2\alpha} \left(\frac{t}{t_{\max}} \right)^{2/3} \right), \quad (30)$$

$$r_3(t) = \frac{3}{2} t_q^{1/3} t^{2/3} \left(1 - \frac{\gamma}{2\alpha} \left(\frac{t}{t_{\max}} \right)^{2/3} \right).$$

where $t_{\max} = t_{\max}(\alpha, \beta, \gamma, \delta_L)$.

3.1 The energy density of GWs

Let us estimate here the amount of gravitational waves produced in the eMD era due to a density perturbation with wavelength q that enters the horizon. At the time of entry t_q , the Hubble comoving volume is $V_q = (4/3)\pi q^3$. Within the current comoving volume of our universe $V_{\text{com}}(t_0) = (4/3)\pi \mathcal{H}^{-3}(t_0)$ there are $\mathcal{H}^{-3}(t_0)/q^3$ volumes with size V_q . At the primordial time t_q the density perturbation in each Hubble patch is characterized by a degree of initial asphericity described by the parameters (α, β, γ) of the deformation tensor and with a distribution of values given by the \mathcal{F}_D probability density. Taking these into account we define the differential number of sources with deformation parameters $(\alpha, \alpha + d\alpha), (\beta, \beta + d\beta), (\gamma, \gamma + d\gamma)$,

$$dN = \frac{V_{\text{com}}(t_0)}{\frac{4}{3}\pi q^3} \mathcal{F}_D(\alpha, \beta, \gamma, \sigma) d\alpha d\beta d\gamma. \quad (31)$$

The power emitted in the form of GWs from each Hubble patch, that encloses a perturbation with a quadrupole tensor Q_{ij} , is

$$\frac{dE_e}{dt} = \frac{G}{5c^5} \sum_{ij} \ddot{Q}_{ij}(t) \ddot{Q}_{ji}(t). \quad (32)$$

Let's define an initial t_i and a final t_f moment of the GW emission. We separate the interval $[t_i, t_f]$ in N intervals of δt size and for each interval we can expand the quadrupole in Fourier series,

$$Q_{ij}(t) = \sum_{n=-\infty}^{\infty} \tilde{Q}_{ij}^N(n\omega_0) e^{-in\omega_0 t}, \quad (33)$$

where $\omega_0 = 2\pi/\delta t$ and $t \in [t_N, t_N + \delta t]$. The \tilde{Q} components are

$$\tilde{Q}_{ij}^N(n\omega_0) = \frac{\omega_0}{2\pi} \int_{t_N}^{t_N + \delta t} Q_{ij}(t) e^{-in\omega_0 t} dt. \quad (34)$$

By taking the continuum limit for ω we transform the last two equations to

$$Q_{ij}(t) = \int \tilde{Q}_{ij}^N e^{i\omega t} d\omega, \quad (35)$$

$$\tilde{Q}_{ij}^N(\omega) = \frac{1}{2\pi} \int_{t_N}^{t_N + \delta t} Q_{ij}(t) e^{-i\omega t} dt. \quad (36)$$

The emitted energy E_e in the time bin $[t_{N_i}, t_{N_i} + \delta t]$ is

$$\begin{aligned} E_e^N &= \frac{2G}{5c^5} \int_{t_N}^{t_N + \delta t} \sum_{ij} \sum_{nm} (in\omega)^3 (-im\omega)^3 \times \tilde{Q}_{ij}^N(n\omega) \tilde{Q}_{ij}^{*N}(m\omega) e^{-i(n-m)\omega t} dt \\ &= \frac{2G}{5c^5} \sum_{ij} \sum_n (n\omega)^6 \tilde{Q}_{ij}^N(n\omega) \tilde{Q}_{ij}^{*N}(n\omega) \delta t. \end{aligned} \quad (37)$$

The above expression has a factor of 2 because we now restrict ourselves in positive n and m since the negative ones contribute equally. In the continuum limit

$$dE_e^N = \frac{4\pi G}{5c^5} \omega^6 \sum_{ij} |\tilde{Q}_{ij}^N|^2 d\omega, \quad (38)$$

and the differential energy emitted per logarithmic interval

$$\frac{dE_e^N}{d \ln \omega} = \frac{4\pi G}{5c^5} \omega^7 \sum_{ij} |\tilde{Q}_{ij}^N(\omega)|^2,$$

within the time bin $[t_N, t_N + \delta t]$. Hence, we find that the infinitesimal energy density today of the differential number of sources with deformation parameters $\{(\alpha, \alpha + d\alpha), (\beta, \beta + d\beta), (\gamma, \gamma + d\gamma)\}$ is

$$dE_{\text{GW}}(\alpha, \beta, \gamma) = \sum_N \frac{1}{1 + z_N} \frac{4\pi G}{5c^5} \omega^7 \sum_{ij} |\tilde{Q}_{ij}^N(\omega)|^2 \frac{V_{\text{com}}(t_0)}{\frac{4\pi}{3} q^3} \mathcal{F}_D(\alpha, \beta, \gamma, \sigma) d\alpha d\beta d\gamma d \ln \omega. \quad (39)$$

We considered that the path of the gravitons, moving in a radial direction is obtained by setting $ds^2 = 0$, and a graviton emitted with an energy E_e is today observed with $E = E_e/(1 + z)$ and frequency $\omega_0 = \omega/(1 + z)$. The cosmological redshift is given by $1 + z = a(0)/a(t_e)$, where we take $a(0) = 1$.

Let us focus here on the GWs emitted from the Hubble patches that experience a pancake collapse of the density perturbation. We expect that these Hubble patches give the dominant contribution to the total GW signal. Inside the Hubble sphere the asphericity will reach the limiting stage of pancake collapse if the time of reheating is sufficiently late, i.e $t_{\text{col}} < t_{\text{rh}}$. Taking as initial time the turning point of maximum expansion $t_i = t_{\text{max}}$ and as final the moment of collapse $t_f = t_{\text{col}}$, we specify the total number of sources as

$$N_{\text{tot}} \simeq \int \frac{V_{\text{com}}(t_0)}{\frac{4\pi}{3} \pi q^3} \Theta(t_{\text{rh}} - t_{\text{col}}(\alpha, \beta, \gamma)) \mathcal{F}_D(\alpha, \beta, \gamma, \sigma) d\alpha d\beta d\gamma. \quad (40)$$

In the unphysical limit $t_{\text{rh}} \rightarrow \infty$ the number of sources is equal to the total number of Hubble patches, $V_{\text{com}}(t_0)/(\frac{4\pi}{3} \pi q^3)$. Separating the duration $[t_{\text{max}}, t_{\text{col}}]$ in N intervals, the differential energy density per observed logarithmic frequency interval and deformation configuration is

$$\begin{aligned} \frac{d\rho_{\text{GW}}(t_0, f_0)}{d\alpha d\beta d\gamma d \ln f_0} &= \sum_N \frac{1}{1 + z_N} \frac{4\pi G}{5c^5} \sum_{ij} |\tilde{Q}_{ij}^N(2\pi f_0(1 + z_N))|^2 \\ &\times (2\pi f_0(1 + z_N))^7 \Theta(t_{\text{rh}} - t_{\text{col}}(\alpha, \beta, \gamma)) \left(\frac{4\pi}{3} q^3\right)^{-1} \mathcal{F}_D(\alpha, \beta, \gamma, \sigma_3). \end{aligned} \quad (41)$$

The f_0 is the frequency parameter today and should not be confused with a specific frequency value. Cosmologists describe the stochastic GW backgrounds by their energy density normalized by the critical energy density of the universe, ρ_{crit} , the so called spectral energy density parameter,

$$\Omega_{\text{GW}}(t, f) \equiv \frac{1}{\rho_{\text{crit}}} \frac{d\rho_{\text{GW}}}{d \ln f}. \quad (42)$$

Its value at the present time reads

$$\begin{aligned} \Omega_{\text{GW}}(t_0, f_0) &= \frac{1}{\rho_{\text{crit}}(t_0)} \int \int \int_{\mathcal{S}} d\alpha d\beta d\gamma \sum_N \frac{1}{1 + z_N} \frac{4\pi G}{5c^5} \sum_{ij} |\tilde{Q}_{ij}^N(2\pi f_0(1 + z_N))|^2 \\ &\times (2\pi f_0(1 + z_N))^7 \Theta(t_{\text{rh}} - t_{\text{col}}(\alpha, \beta, \gamma, \sigma)) \left(\frac{4\pi}{3} q^3\right)^{-1} \mathcal{F}_D(\alpha, \beta, \gamma, \sigma). \end{aligned} \quad (43)$$

where the integration takes place over the parameters space \mathcal{S} (27). Eq. (43) is the *main result of this work*. Apparently, the total energy density parameter today is given by the integral $\Omega_{\text{GW}}(t_0) = \int \Omega_{\text{GW}}(t_0, f_0) d \ln f_0$. In the following we will apply our result estimating the contribution to the GW from regions that collapse into PBHs and the entire contribution from all the regions that experience a pancake collapse before the reheating of the universe.

4 Estimation of the GW signal amplitude and spectrum

We can now proceed and calculate the sum of the square of the quadrupole moments. In practice it turned out to be simpler to directly calculate the Fourier transform of $\ddot{Q}_{ij}(t)$. Using Eqs. (28), (29), (30) and (36) for a time bin $[t_1, t_2]$ we get,

$$\omega^6 \sum_{ij} |\tilde{Q}_{ij}^N(\omega)|^2 = \frac{1}{54\pi^2} \frac{t_q^{4/3} t_1^{4/3}}{t_{\max}^{8/3}} M^2 \left[1 + \left(\frac{\beta}{\alpha}\right)^4 + \left(\frac{\gamma}{\alpha}\right)^4 - \left(\frac{\gamma}{\alpha}\right)^2 - \left(\frac{\beta}{\alpha}\right)^2 \left(1 + \left(\frac{\gamma}{\alpha}\right)^2\right) \right] \times \left| \text{Ei} \left[\frac{1}{3}, i\omega t_1 \right] - \left(\frac{t_2}{t_1}\right)^{2/3} \text{Ei} \left[\frac{1}{3}, i\omega t_2 \right] \right|^2. \quad (44)$$

For the expression of Eq. (43) to be absolutely correct, N must be large i.e., we should partition the time interval $[t_{\max}, t_{\text{col}}]$ to a large number of small time intervals. The reason for having to do that instead of taking the Fourier transform for the full interval is because frequencies produced at different times are redshifted by different amounts as they reach our detectors today. As a first approximation we will consider only one interval (i.e., $N = 1$) and we will consider as if the GWs were emitted instantaneously at t_{col} . This is a very good approximation since $t_{\text{col}} = 2^{3/2} t_{\max}$ and t_{\max} are relatively close to each other, and therefore the introduced horizontal error in the frequency is at most a factor of 2. By use of Eq. (44) within this ‘‘average’’ approximation, Eq. (43) is recast into

$$\Omega_{\text{GW}}(t_0, f_0) = \frac{1}{\rho_{\text{crit}}} \left(\frac{4\pi}{3} q^3\right)^{-1} \frac{4\pi G}{5c^5} \frac{2\pi f_0}{54\pi^2} M^2 \sigma^2 \int \int \int_{\mathcal{S}} d\alpha d\beta d\gamma \left(\frac{2\alpha}{\alpha + \beta + \gamma}\right)^2 \times \left[1 + \left(\frac{\beta}{\alpha}\right)^4 + \left(\frac{\gamma}{\alpha}\right)^4 - \left(\frac{\gamma}{\alpha}\right)^2 - \left(\frac{\beta}{\alpha}\right)^2 \left(1 + \left(\frac{\gamma}{\alpha}\right)^2\right) \right] \times \left| \text{Ei} \left[\frac{1}{3}, it_{\max}(\alpha, \beta, \gamma, \sigma) 2\pi f_0 (1 + z_{\text{col}}(\alpha, \beta, \gamma, \sigma)) \right] - 2 \text{Ei} \left[\frac{1}{3}, it_{\text{col}}(\alpha, \beta, \gamma, \sigma) 2\pi f_0 (1 + z_{\text{col}}(\alpha, \beta, \gamma, \sigma)) \right] \right|^2 \times \Theta(t_{\text{rh}} - t_{\text{col}}(\alpha, \beta, \gamma, \sigma)) \mathcal{F}_{\text{D}}(\alpha, \beta, \gamma, \sigma_3). \quad (45)$$

The above equation is the one that we use to derive our numerical results.

The estimation of the $\Omega_{\text{GW}}(t_0, f_0)$ requires the integration over the parameter space (α, β, γ) . The step function $\Theta(t_{\text{rh}} - t_{\text{col}}(\alpha, \beta, \gamma))$ is modulated by t_{col} and its value has also a probability distribution. Also the expectation value of the expression $\langle ((\alpha + \beta + \gamma)/\alpha)^{3/2} \rangle$ has a very weak sensitivity on σ and hence the expectation value of the key moments of maximum expansion and collapse scale as $\langle t_{\max} \rangle, \langle t_{\text{col}} \rangle \propto \sigma^{-3/2}$. The step function condition $t_{\text{rh}} > t_{\text{col}}(\alpha, \beta, \gamma, \sigma)$ can be translated into an upper bound for the reheating temperature as

$$T_{\text{rh}} \lesssim 0.2 \left(\frac{\alpha \sigma}{\alpha + \beta + \gamma}\right)^{3/4} \left(\frac{M_{\odot}}{M}\right)^{1/2} \left(\frac{g_*}{106.75}\right)^{-1/4} \text{GeV}, \quad (46)$$

where M_{\odot} is the solar mass. If this upper bound is violated, some regions will not collapse into a pancake before the transition to the radiation phase. For t_{rh} not very close to $\langle t_{\text{col}} \rangle$ the Θ step function does not reduce the parameter space \mathcal{S} to modify essentially the integral (45).

The redshift experienced by the GW emitted at the collapse moment has also a probability distribution and is given by the expression

$$1 + z_{\text{col}} = \frac{1 + z_{\text{rh}}}{(6\pi G \rho_{\text{rh}})^{1/3} t_{\text{col}}^{2/3}}. \quad (47)$$

Also, the comoving radius of the the perturbation at the time of horizon entry, q , corresponds to the wavenumber,

$$\begin{aligned} q^{-1}(M, T_{\text{rh}}) &= \left(\frac{3M(1+z_{\text{rh}})^3}{4\pi\rho_{\text{rh}}} \right)^{-1/3}, \\ &\simeq 1.2 \times 10^{10} \left(\frac{T_{\text{rh}}}{10^{10}\text{GeV}} \right)^{\frac{1}{3}} \left(\frac{M}{M_{\odot}} \right)^{-\frac{1}{3}} \text{Mpc}^{-1}, \end{aligned} \quad (48)$$

where $\rho_{\text{rh}} = \pi^2 g_* T_{\text{rh}}^4 / 30$ is the energy density at the time of reheating and the redshift z_{rh} can be easily found using the conservation of entropy.

4.1 GWs associated with the PBH formation

We will first focus on the collapsing configurations that lead to formation of PBHs. According to the hoop conjecture [43, 44] a black hole forms when the circumference in every direction is approximately smaller than 2π times the Schwarzschild radius, $r_s = 2GM/c^2$. The hoop \mathcal{C} of the pancake is given by the circumference of an ellipse $\mathcal{C} = 4r_3(t_{\text{col}})E(e)$ where $E(e)$ is the complete elliptic integral of the second kind and e the eccentricity of the pancake,

$$e = \sqrt{1 - \left(\frac{r_2(t_{\text{col}})}{r_3(t_{\text{col}})} \right)^2} = \sqrt{1 - \left(\frac{\alpha - \beta}{\alpha - \gamma} \right)^2}. \quad (49)$$

The hoop conjecture for the ellipsis reads $\mathcal{C} \lesssim 2\pi r_s$, or

$$h(\alpha, \beta, \gamma) \equiv \frac{\mathcal{C}}{2\pi r_s} = \frac{2}{\pi} \frac{\alpha - \gamma}{\alpha^2} E \left(\sqrt{1 - \left(\frac{\alpha - \beta}{\alpha - \gamma} \right)^2} \right) \lesssim 1. \quad (50)$$

The number of GW sources associated with PBH formation is given by a subspace of (α, β, γ) parameter space,

$$N_{\text{PBH}} = \frac{V_{\text{com}}}{\frac{4}{3}\pi q^3} \int \Theta(1 - h(\alpha, \beta, \gamma)) \Theta(t - t_{\text{col}}(\alpha, \beta, \gamma, \sigma)) \mathcal{F}_D(\alpha, \beta, \gamma, \sigma) d\alpha d\beta d\gamma,$$

that fulfills the hoop criterion. Actually the PBH formation criterion $h < 1$ implies

$$\alpha - \gamma \lesssim \frac{\pi}{2} \alpha^2 = \frac{\pi}{2} \mathcal{O}(\sigma_3^2), \quad (51)$$

thus it is $\alpha - \gamma \sim \mathcal{O}(\sigma_3^2)$, $\alpha - \beta \sim \mathcal{O}(\sigma_3^2)$ and $\beta - \gamma \sim \mathcal{O}(\sigma_3^2)$. We define the ratio ϵ ,

$$\frac{\alpha - \gamma}{\alpha} \sim \frac{\alpha - \beta}{\alpha} \sim \frac{\sigma_3^2}{\alpha} \equiv \epsilon < 1. \quad (52)$$

Since $\alpha \sim \sigma_3$, for $\sigma_3 \ll 1$, it should be also $\epsilon \ll 1$. Therefore we can expand Eq. (45) with respect to the small parameter $\epsilon = \sigma_3^2/\alpha$ up to quadratic order, approximating the brackets of Eq. (45) as $4\epsilon^2$, and recast the expression for the energy density parameter in the form,

$$\begin{aligned} \Omega_{\text{GW}}^{(\text{PBH})}(t_0, f_0) &\simeq \frac{1}{\rho_{\text{crit}}} \frac{4\pi G}{5c^5} \frac{2\pi f_0}{54\pi^2} M^2 \left(\frac{4\pi}{3} q^3 \right)^{-1} \frac{4}{25} \sigma^6 \times \\ &\int \int \int_{\mathcal{S}_{\text{PBH}}} d\alpha d\beta d\gamma \left(\frac{2\alpha}{\alpha + \beta + \gamma} \right)^2 \frac{1}{\alpha^2} \\ &\left| \text{Ei} \left[\frac{1}{3}, it_{\text{max}}(\alpha, \beta, \gamma, \sigma) 2\pi f_0 (1 + z_{\text{col}}(\alpha, \beta, \gamma, \sigma)) \right] \right. \\ &\left. - 2\text{Ei} \left[\frac{1}{3}, it_{\text{col}}(\alpha, \beta, \gamma, \sigma) 2\pi f_0 (1 + z_{\text{col}}(\alpha, \beta, \gamma, \sigma)) \right] \right|^2 \\ &\times \Theta(t_{\text{rh}} - t_{\text{col}}(\alpha, \beta, \gamma, \sigma)) \mathcal{F}_D(\alpha, \beta, \gamma, \sigma_3), \end{aligned} \quad (53)$$

where the \mathcal{S}_{PBH} is selected by the hoop-condition step function $\Theta(1 - h)$. In particular, the constraint $h \lesssim 1$ implies that only a subspace of $-\infty < \alpha < \infty$, $-\infty < \beta < \alpha$ and $-\infty < \gamma < \beta$ leads to PBH formation, that in terms of new variables $x = (\alpha + \beta + \gamma)/3$, $y = (\alpha - 2\beta + \gamma)/4$ and $z = (\alpha - \gamma)/2$ reads $0 < x$, $-x^2/4 < y < x^2/4$, $2|y| < z < x^2/2$ in the circular limit ($e = 0$) and $0 < x$, $-x^2\pi/8 < y < x^2\pi/8$, $2|y| < z < x^2\pi/4$ in the eccentric limit ($e = 1$) [51]. In the left panel of Fig. 2 the GW signal is depicted for two σ values after computing the integral of Eq. (53), involving the Doroshkevich probability distribution of non spherical perturbations, over the subspace \mathcal{S}_{PBH} in the eccentric limit and for several hundreds of frequency values over the frequency band of interest. For different σ values a different integration interval is found; note that as the σ decreases $\langle 1/\alpha^2 \rangle$ also decreases due to the shrinking of the parameter space that realize PBH formation.

In principle we should evaluate the quadrupole induced GW signal not up to t_{col} but up to t_{BH} the first moment where the hoop conjecture was satisfied. Obviously $t_{\text{col}} > t_{\text{BH}}$. In our approximation we have used as the end time of emission t_{col} and not t_{BH} . However we will argue that the two times are very close to each other, and therefore using t_{col} instead of t_{BH} does not introduce any substantial error. Given that at any time t between t_{max} and t_{col} the circumference of the ellipsoid is given by $C = 4r_3(t)E(e)$, we can rewrite the condition for the hoop conjecture of Eq. (50) for time t as

$$\frac{2}{\pi} \xi \frac{\alpha - \xi\gamma}{\alpha^2} E(e) \lesssim 1, \quad (54)$$

where $\xi = (t/t_{\text{col}})^{2/3}$. For $\xi = 1$, one recovers Eq. (50). In the circular limit $E(0) = \pi/2$ and therefore the above equation becomes

$$\xi \frac{\alpha - \xi\gamma}{\alpha^2} \lesssim 1. \quad (55)$$

This equation must be satisfied in order to form a black hole. Given that ξ takes values within $[0.5, 1]$ for $t_{\text{BH}} < t < t_{\text{col}}$, α and γ are $\mathcal{O}(\sigma_3)$ while $\alpha - \gamma \sim \mathcal{O}(\sigma_3^2)$, one realizes from the above equation that it cannot be satisfied unless ξ is fine tuned close to 1 in order to make $\alpha - \xi\gamma \sim \mathcal{O}(\sigma_3^2)$. If ξ is not very close to 1, $\alpha - \xi\gamma \sim \mathcal{O}(\sigma_3)$ and the above equation cannot be satisfied. A similar argument works also for the eccentric limit leading to the same conclusion $t_{\text{BH}} \simeq t_{\text{col}}$.

4.2 GWs not necessarily associated with PBH formation

Let us consider now the entire GW contribution from the overdensities that enter the horizon at the time of entry t_q , evolve and collapse into pancake shape before the reheating of the universe. Here we include the full parameter space for α, β, γ , Eq. (27), contrary to the previous case (51), where we limit ourselves to configurations that collapse into PBHs. There is no surprise that this case leads to larger GW signals. This is easily understood from the fact that PBH formation requires small deviations from sphericity and therefore smaller parameter space and smaller quadrupole moment which is essential for GW generation. On the contrary collapsing overdensities which are too asymmetric to form PBHs have larger quadrupole moments and larger parameter space to explore. Now unlike the case of PBH formation the difference between the deformation factors is of the order of the variance value, $\alpha - \gamma = \mathcal{O}(\sigma_3)$ (and not $\mathcal{O}(\sigma_3^2)$).

Therefore we find the spectral energy density parameter of the GWs emitted by the Hubble patches that experience a pancake collapse after computing the full integral in Eq. (45) over the parameter space \mathcal{S} given by Eq. (27). We implement the computation after an integration for several hundreds of discrete frequency values over a frequency band of interest. For different values for M , T_{rh} and σ our numerical results are plotted in Figs. 2-4.

The amplitude of the GW signal is σ^2 dependent times the integral of the Doroshkevich probability distribution over the \mathcal{S} parameter space which also depends on σ . To get a better

understanding, the part of the integrand in Eq. (45),

$$\left[1 + \left(\frac{\beta}{\alpha}\right)^4 + \left(\frac{\gamma}{\alpha}\right)^4 - \left(\frac{\gamma}{\alpha}\right)^2 - \left(\frac{\beta}{\alpha}\right)^2 \left(1 + \left(\frac{\gamma}{\alpha}\right)^2\right) \right] \left(\frac{2\alpha}{\alpha + \beta + \gamma}\right)^2, \quad (56)$$

yields a σ dependence roughly inversely proportional to σ . Hence the GW signal has a nearly linear dependence on σ . By inspecting the frequency dependent terms in Eq. (45) and after rewriting $2\pi f_0$ as $2\pi f/(1+z_{\text{col}})$ we see that the product $\omega \left| \text{Ei} \left[\frac{1}{3}, it_{\text{max}}\omega \right] - 2\text{Ei} \left[\frac{1}{3}, 2\sqrt{2}it_{\text{max}}\omega \right] \right|^2$ features a peak at $\omega \sim 1/t_{\text{max}}$ with a value $\sim 1/t_{\text{max}}$, where $\langle t_{\text{max}} \rangle \simeq 0.17 \sigma^{-3/2} t_q$. The actual maximum of the GW spectrum is specified only after computing the integral in Eq. (45) and the peak frequency is given approximately by the relation

$$f_{\text{peak}}(M, T_{\text{rh}}) \simeq 2.5 \times 10^{-8} \left(\frac{M}{M_{\odot}}\right)^{-1/3} \left(\frac{T_{\text{rh}}}{\text{GeV}}\right)^{1/3} \text{ Hz}. \quad (57)$$

After normalizing with benchmark values, we write the expression for the spectral energy density parameter of the GWs at the peak frequency f_{peak} ,

$$\Omega_{\text{GW}}(f_{\text{peak}}, t_0) \sim 1.9 \times 10^{-7} \left(\frac{M}{M_{\odot}}\right)^{2/3} \left(\frac{T_{\text{rh}}}{\text{GeV}}\right)^{4/3} \left(\frac{\sigma}{0.1}\right) \quad (58)$$

for $t_{\text{rh}} > t_{\text{col}}(\sigma, M)$.

We stress that the plots in Fig. 2-4 are produced after performing the full triple integral in Eq.(45) without assuming any approximation.

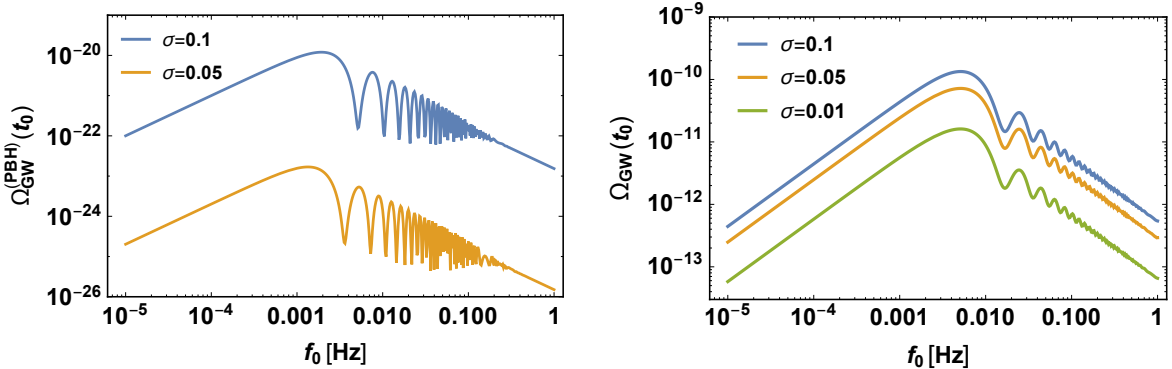


Figure 2: *Left panel.* The GW signal produced only by the regions that collapse into PBH for different σ values and reheating temperature $T_{\text{rh}} = 10^4$ GeV. The horizon mass is $M = 10^{-12} M_{\odot}$. *Right panel.* The entire GW signal for the same horizon mass and temperature.

The GW spectrum we observe today scales as $\Omega(t_0, f_0) \propto f_0$ in the IR regime and the envelope of the oscillating spectrum falls as $\Omega(t_0, f_0) \propto f_0^{-1}$ in the UV. The peak, which is the peak of the first oscillation, falls much faster, roughly like f_0^{-3} , see Fig. 2. This is a distinct feature of the GWs produced during eMD from a monochromatic source. We add that the GW signal produced during an eMD era (43) has also a different dependence on $\sigma = \sqrt{\mathcal{P}_{\delta}}$ and different amplitude compared to the GW signal produced during the radiation domination era [23–25] or just before the transition to the radiation era [31, 32].

5 GWs and the PBH abundance

In the absence of pressure even minute perturbations will evolve, and in the spherical limit, will collapse into a black hole. PBH production during matter era has been first examined in Ref. [56, 57]. Ref. [51] examined the PBH production in a matter dominated universe and

considered the non-spherical effects in gravitational collapse. The production probability of PBH is given by

$$\beta_0 = \int_0^\infty d\alpha \int_{-\infty}^\alpha d\beta \int_{-\infty}^\beta d\gamma \Theta(1 - h(\alpha, \beta, \gamma)) \mathcal{F}_D(\alpha, \beta, \gamma). \quad (59)$$

For small σ the PBH production rate β_0 tends to be proportional to σ^5 ,

$$\beta_0(\sigma) = 0.056 \sigma^5. \quad (60)$$

This expression has been derived with semi-analytical calculations and applies for $0.005 \lesssim \sigma \lesssim 0.2$, whereas for $\sigma \lesssim 0.005$ the PBH production rate is modified if there is an angular momentum in the collapsing region [58]. For such a small σ however, the GW signal becomes negligibly small for the sensitivity of the operating and designed GW detectors. The PBH dark matter fractional abundance is

$$f_{\text{PBH}} \equiv \frac{\Omega_{\text{PBH}}}{\Omega_{\text{DM}}} \simeq 1.3 \times 10^{19} \gamma_{\text{M}} \beta_0 \left(\frac{T_{\text{rh}}}{10^{10} \text{ GeV}} \right). \quad (61)$$

By definition the fractional abundance is equal or less than one but in the largest part of the mass spectrum there are stringent upper bounds on $\Omega_{\text{PBH,max}}/\Omega_{\text{DM}}$ due to observational constraints, see Fig. 5. The maximum value $\Omega_{\text{PBH,max}}/\Omega_{\text{DM}} = 1$ is possible in the mass range $M_{\text{PBH}} \sim 10^{-15} - 10^{-10} M_\odot$. The γ_{M} that appears in Eq. (61) is the fraction of the horizon mass that collapses into PBH during the matter domination era. It is a numerical factor which depends on the details of gravitational collapse and it can admit values possibly from $\gamma_{\text{M}} \sim 10^{-4}$ up to $\gamma_{\text{M}} \sim 1$ [59, 60]. Note that PBHs form mostly by spherical collapse and γ_{M} is not related with the asphericity developed in other Hubble patches that dominate the GWs emission.

According to Eq. (61) the variance (60) is bounded from above. When the upper bound on σ is saturated the PBH abundance maximizes. Several observational experiments determine the $\Omega_{\text{PBH,max}}$ in a wide range for the mass parameter M_{PBH} labeled in Fig. 5. Light PBHs are constrained from the extra galactic gamma-ray background (EGB) [61–65], as well as from e^\pm annihilation in the galactic center (GC) and positron constraints (V) [66]. Black holes of mass above 10^{17} g are subject to gravitational lensing constraints [67–69], given by Subaru (HSC), Ogle (O), EROS (E) and MACHO (M), microlensing of supernova (SN) and others. The CMB anisotropies measured by Planck (PA) constrains the PBH with mass above 10^{33} g [70–75]. At the large mass region there are also constraints from accretion limits in X-ray and radio observations [76] and X-ray binaries (XB) [77]. There are also dynamical limits from disruption of wide binaries (WB) [78], and survival of star clusters in Eridanus II (Er) [79]. Advanced LIGO/Virgo searches for compact binary systems with component masses in the range $0.2 - 1 M_\odot$ find no viable GW candidates [80]. The non-observation of the stochastic GW background (GWB) from PBH mergers from LIGO/Virgo constrains PBHs with mass in the range $1 - 10^2 M_\odot$ for the monochromatic mass function [81, 82]. However disruption of PBH binaries might have been underestimated and it is probable that the merger rate might be smaller thus invalidating the aforementioned constraint Ref. [83]. Finally second order tensor perturbations (GW2) generated by scalar perturbations already constrain the abundance of PBH masses approximately in the range $10^{-3} - 1 M_\odot$. For a recent update on the PBH constraints see Ref. [77]. What is of special interest in the present work is that the PTA bound² on the second order tensors (GW2) [3, 85–87], depicted in Fig. 5, does not apply as it is if a late reheating takes place. Instead, a significant PBH dark matter component can be consistent with the current pulsar timing data if produced during eMD.

²We mention that the NANOGrav Collaboration has recently published an evidence of an isotropic stochastic process [84].

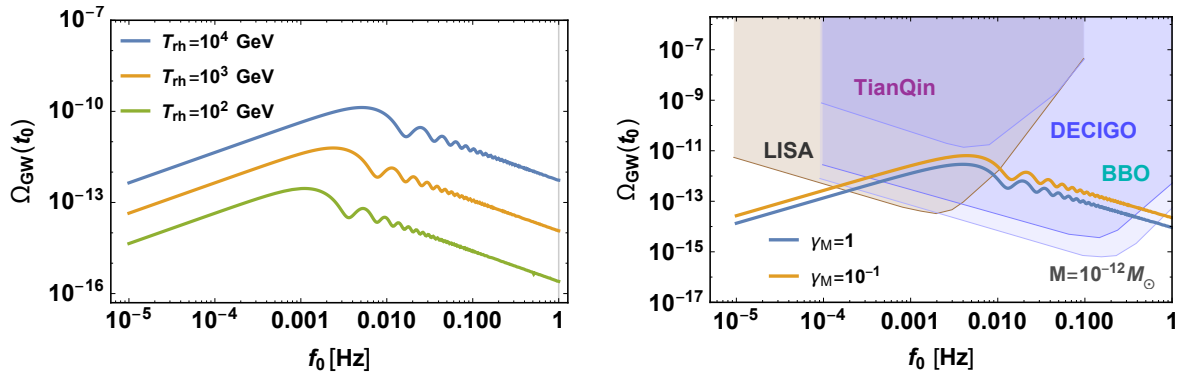


Figure 3: *Left panel.* The GW signal for $\sigma = 0.1$ and horizon mass $M = 10^{-12} M_\odot$ for three different reheating temperatures. *Right Panel.* The maximum GW signal in the LISA-BBO frequency band for the PBH dark matter scenario for two different γ_M values. For $\gamma_M = 1$ it is $\sigma = 0.0047$ and for $\gamma_M = 0.1$ it is $\sigma = 0.0071$ so that $\Omega_{\text{PBH}} = \Omega_{\text{DM}}$; the reheating temperature is chosen to be $T_{\text{rh}} = T_{\text{col}}/2$, that is 4.8×10^3 GeV and 6.5×10^3 GeV respectively. The horizon and the PBHs have masses $M = 10^{-12} M_\odot$ and $M_{\text{PBH}} = \gamma_M M$ respectively.

5.1 PBH as the entire dark matter of the universe

In the mass window $M_{\text{PBH}} = 10^{-15} - 10^{-10} M_\odot$ the PBH abundance can reach its maximum value, i.e., it can account for 100% of the dark matter abundance. If PBHs constitute a significant fraction of the total dark matter then a GW counterpart must exist that can be tested by the scheduled Laser Interferometer Space Antenna (LISA) [4], as well as by other space-based proposed experiments such as DECIGO [7, 8], BBO [88], TianQin [6], and Taiji [5]. For (see Eq. (46))

$$T_{\text{rh}} \lesssim 5 \times 10^5 \text{ GeV } \sigma^{3/4} \left(\frac{M}{10^{-12} M_\odot} \right)^{-1/2} \quad (62)$$

our result, given by Eq. (43), applies and gives the GW spectrum. The GW signal is generally found with a different amplitude compared to the signal produced during radiation dominated era and the peak frequency shifted towards smaller values as the reheating temperature decreases (see Fig. 3). In view of the γ_M uncertainties, we plot in Fig. 3 the GW signal for two different γ_M parameters in the LISA-BBO frequency band. For the PBH dark matter scenario, smaller γ_M parameter values increase the GWs amplitude. The peak frequency of the signal is the signature of the PBH dark matter scenario in cosmologies with low reheating temperatures.

5.2 PBH with solar and sub-solar masses

Besides the recent result of NANOGrav Collaboration [84], PTA experiments rule out the existence of practically any PBH with mass $M_{\text{PBH}} = \mathcal{O}(10^{-3} - 1) M_\odot$ [3, 85–87], as depicted in Fig. 5. However, the depicted PTA bound on the second order tensors (GW2) has been derived assuming a radiation dominated era. For reheating temperature (see Eq. (62)) less than $T_{\text{rh}} < 10^3 \sigma^{3/4} (M_\odot/M)^{1/2}$ MeV, GWs that are produced during eMD might avoid the severe GW2 constraint on the PBH abundance, depicted in Fig. 5. Hence, at that mass range $10^{-3} - 1 M_\odot$ the PBH abundance can be a non negligible fraction of the total dark matter abundance, even up to few % according to the bounds from EROS and MACHO microlensing experiments, without overproducing GWs. Let us note that a further motivation in this mass range is the intriguing event [89] and the recent evidence for a stochastic GW background [84].

As an example, let us take $\Omega_{\text{PBH}}/\Omega_{\text{DM}} = 5\%$ for $M_{\text{PBH}} = 0.1 M_\odot$ and $\gamma_M = 1$. According to Eqs. (60), and (61) such an abundance is obtained for $\sigma = 0.023$. For $T_{\text{rh}} = 1/2 T_{\text{col}} = 87$ MeV, these parameters yield a GW signal that has a maximal amplitude $\Omega_{\text{GW}}(t_0, f_{\text{peak}}) = 1.4 \times 10^{-10}$ at the peak frequency $f_{\text{peak}} = 2.4 \times 10^{-8}$ Hz, see Eq. (58) and (57), and this value is fully compatible with the current PTA constraints. In Fig. 4 the GW signal has been plotted

together with a second case that yields $\Omega_{\text{PBH}}/\Omega_{\text{DM}} = 0.1\%$. Near future PTA experiments, SKA [90,91] and FAST [92], can test the PBHs scenarios in eMD cosmologies with low reheating temperatures and with mass in the range between the earth and the sun.

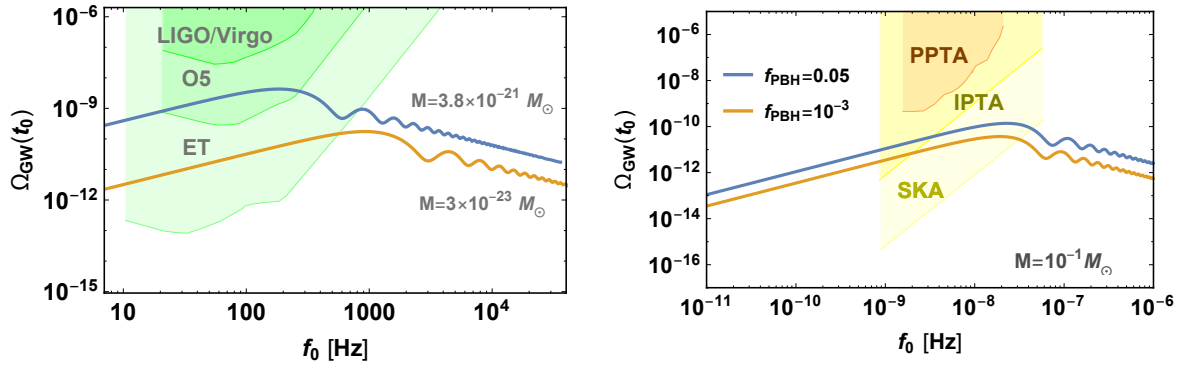


Figure 4: *Left panel.* The GW signal in the LIGO/Virgo and Einstein Telescope frequency range for promptly evaporating PBHs and $\sigma = 0.1$, $T_{\text{rh}} = 2 \times 10^9$ GeV for two horizon masses, $M = 3.8 \times 10^{-21} M_{\odot}$ and $M = 3 \times 10^{-23} M_{\odot}$. The BBN constraints are evaded for $10^{-4} \lesssim \gamma_{\text{M}} \lesssim 2 \times 10^{-2}$. If these PBHs leave behind a remnant with mass κM_{Pl} it can constitute a significant part of the dark matter in the universe for $\kappa \gg 1$. *Right Panel.* The GW signal in the PTA frequency range, for horizon mass $M = 10^{-1} M_{\odot}$ and for two fractional abundances for the associated PBHs 5% and 0.1% and for $\gamma_{\text{M}} = 1$. The σ value corresponds to 0.023 (upper curve) and 0.012 (lower curve) and the reheating temperature is chosen to be $T_{\text{rh}} = T_{\text{col}}/2$, that is 87 and 53 MeV respectively.

5.3 Ultra light PBHs

Lighter PBHs are associated with GW production in larger frequencies. Currently the LIGO-Virgo probes the frequency band around $f = 100$ Hz. According to Eq. (57) GWs will be produced with that frequency range if PBHs have mass $\gamma_{\text{M}} M_{\text{PBH}} \sim 10^{-20} M_{\odot}$ ($T_{\text{rh}}/10^9 \text{ GeV}$). LIGO-Virgo, as well as the Einstein Telescope [9], can hence detect GWs associated with PBHs with mass $10^{-20} M_{\odot}$ or less, see e.g. [29, 93]. PBHs with very light masses are anticipated to Hawking radiate and evaporate in timescales less than the age of the universe for $M_{\text{PBH}} < 10^{-16} M_{\odot}$. Due to the energetic Hawking radiation, strong constraints on their abundance have been placed [60, 77]. However, the scenario of mini PBHs is interesting due to the theoretical expectation that black holes might not evaporate into nothing but leave behind a stable state, called black hole remnant. PBH remnants can actually comprise the entire dark matter of the universe [49, 94, 95]. For PBH formation during a matter domination era the fractional abundance of the PBH remnants is [49],

$$\frac{\Omega_{\text{rem}}}{\Omega_{\text{DM}}} \simeq 3 \times 10^{-6} \kappa \left(\frac{\beta_0}{10^{-9}} \right) \left(\frac{M}{10^{10} \text{ g}} \right)^{-1} \left(\frac{T_{\text{rh}}}{10^{10} \text{ GeV}} \right), \quad (63)$$

where $M_{\text{rem}} = \kappa M_{\text{Pl}}$ is the mass of the remnant. PBHs with mass less than about 10^9 grams are free from the BBN observational constraints [77]. The maximum value of the GW signal is $\Omega_{\text{GW}} \sim 4.5 \times 10^{-22} \sigma (T_{\text{rh}}/\text{GeV})^2 (f_{\text{peak}}/\text{Hz})^{-2}$. Assuming small values for the γ_{M} parameter the GW signal can be strong enough to be detectable by LIGO-Virgo without violating BBN constraints. Particular combinations of κ and γ_{M} values can also realize the PBH remnant dark matter scenario and near future experiments could set constraints on the anticipated GW signal, see Fig. 4.

6 Conclusions

In this work we examined the gravitational waves produced during an early matter domination era due to the non-spherical evolution of the primordial density perturbations. We applied

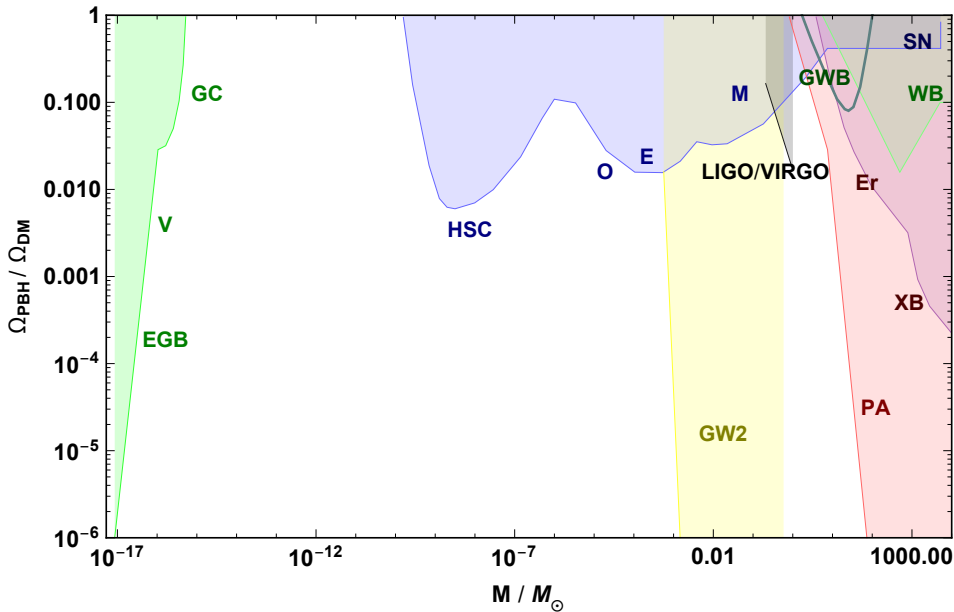


Figure 5: The observational bounds on $\Omega_{\text{PBH}}/\Omega_{\text{DM}}$ [77], as described in the text. Note that the depicted GW2 bound does not apply in our case.

the Zel’dovich approximation to describe the nonlinear evolution of the density perturbation and derived the expression for the GW spectrum by exerting the quadrupole piece. To our knowledge, this is a novel result since this is the first time where this non-perturbative method is used in order to estimate the GW signal. After a series of analytical steps we estimate the GW signal numerically, performing the full integration of the triple integral in Eq. (45). This paper also serves as a proof of concept. Within our method it is allowed to make a full very precise non-perturbative estimate increasing N the number of time intervals which we partition the time interval $[t_{\text{max}}, t_{\text{col}}]$.

We have found distinct features for the GW signal which can distinguish it from GW signals of a radiation domination scenario: it has a different amplitude, peaked at different frequencies shifted towards smaller values as the reheating temperature decreases and with different power-law scaling compared to the radiation domination case. Turning to the PBH counterpart we also find different predictions. PBHs can be the dark matter of the universe in the mass region $M_{\text{PBH}} \sim 10^{-15} - 10^{-11} M_{\odot}$ with the associated GWs signal being inside the sensitivity curve of the LISA curve. In addition, PBHs in the solar mass range or less, $M_{\text{PBH}} \sim 10^{-3} - 1 M_{\odot}$, can have a significant abundance without violating the existing PTA constraints (where models of PBH formed in radiation domination are subjected to), if the reheating temperature is sufficient low.

We plan to extend our work also by studying the GW signal produced from overdensities that did not form black holes as they evolve from a collapsed structure to a virialized halo. This signal could be as strong as the one estimated here and it could have different spectral characteristics which could facilitate the identification of a potential signal easier.

It is expected that gravitational-wave astronomy will make a significant progress in the next decades. This could allow us to probe and test non-thermal early universe histories as well as PBH dark matter scenarios. In addition, the results of the present work contribute to the understanding of the properties and variations of the presumably present stochastic gravitational wave background.

Acknowledgments

I.D. would like to thank CP3 Origins, University of Southern Denmark for hospitality during the early stages of this work. The research work of I.D. was supported by the Hellenic Foundation

for Research and Innovation (H.F.R.I.) under the "First Call for H.F.R.I. Research Projects to support Faculty members and Researchers and the procurement of high-cost research equipment grant" (Project Number: 824).

References

- [1] B. P. Abbott *et al.* [LIGO Scientific and Virgo], Phys. Rev. Lett. **116** (2016) no.6, 061102 [[gr-qc/1602.03837](#)].
- [2] B. P. Abbott *et al.* [LIGO Scientific and Virgo], "Upper Limits on the Stochastic Gravitational-Wave Background from Advanced LIGO's First Observing Run," Phys. Rev. Lett. **118** (2017) no.12, 121101 [erratum: Phys. Rev. Lett. **119** (2017) no.2, 029901] [[gr-qc/1612.02029](#)].
- [3] Z. C. Chen, C. Yuan and Q. G. Huang, "Pulsar Timing Array Constraints on Primordial Black Holes with NANOGrav 11-Year Dataset," Phys. Rev. Lett. **124** (2020) no.25, 251101 [[astro-ph.CO/1910.12239](#)].
- [4] P. Amaro-Seoane *et al.* [LISA], "Laser Interferometer Space Antenna," [[astro-ph.IM/1702.00786](#)].
- [5] W. H. Ruan, Z. K. Guo, R. G. Cai and Y. Z. Zhang, "Taiji program: Gravitational-wave sources," Int. J. Mod. Phys. A **35** (2020) no.17, 2050075 [[gr-qc/1807.09495](#)].
- [6] J. Luo *et al.* [TianQin], "TianQin: a space-borne gravitational wave detector," Class. Quant. Grav. **33** (2016) no.3, 035010 [[astro-ph.IM/1512.02076](#)].
- [7] N. Seto, S. Kawamura and T. Nakamura, "Possibility of direct measurement of the acceleration of the universe using 0.1-Hz band laser interferometer gravitational wave antenna in space," Phys. Rev. Lett. **87** (2001), 221103 [[astro-ph/astro-ph/0108011](#)].
- [8] S. Sato, S. Kawamura, M. Ando, T. Nakamura, K. Tsubono, A. Araya, I. Funaki, K. Ioka, N. Kanda and S. Moriwaki, *et al.* "The status of DECIGO," J. Phys. Conf. Ser. **840** (2017) no.1, 012010
- [9] B. Sathyaprakash, M. Abernathy, F. Acernese, P. Ajith, B. Allen, P. Amaro-Seoane, N. Andersson, S. Aoudia, K. Arun and P. Astone, *et al.* "Scientific Objectives of Einstein Telescope," Class. Quant. Grav. **29** (2012), 124013 [erratum: Class. Quant. Grav. **30** (2013), 079501] [[gr-qc/1206.0331](#)].
- [10] M. Sasaki, T. Suyama, T. Tanaka and S. Yokoyama, "Primordial black holes—perspectives in gravitational wave astronomy," Class. Quant. Grav. **35** (2018) no.6, 063001 [[astro-ph.CO/1801.05235](#)].
- [11] S. Kuroyanagi, T. Chiba and T. Takahashi, "Probing the Universe through the Stochastic Gravitational Wave Background," JCAP **11** (2018), 038 [[astro-ph.CO/1807.00786](#)].
- [12] N. Christensen, "Stochastic Gravitational Wave Backgrounds," Rept. Prog. Phys. **82** (2019) no.1, 016903 [[gr-qc/1811.08797](#)].
- [13] C. Caprini and D. G. Figueroa, "Cosmological Backgrounds of Gravitational Waves," Class. Quant. Grav. **35** (2018) no.16, 163001 [[astro-ph.CO/1801.04268](#)].
- [14] P. M. Sa and A. B. Henriques, "Gravitational wave generation in loop quantum cosmology," Phys. Rev. D **85** (2012), 024034 [[gr-qc/1108.0079](#)].
- [15] S. Matarrese, O. Pantano and D. Saez, "A General relativistic approach to the nonlinear evolution of collisionless matter," Phys. Rev. D **47** (1993), 1311-1323
- [16] S. Matarrese, O. Pantano and D. Saez, "General relativistic dynamics of irrotational dust: Cosmological implications," Phys. Rev. Lett. **72** (1994), 320-323 [[astro-ph/astro-ph/9310036](#)].
- [17] S. Matarrese, S. Mollerach and M. Bruni, "Second order perturbations of the Einstein-de Sitter universe," Phys. Rev. D **58** (1998), 043504 [[astro-ph/astro-ph/9707278](#)].
- [18] H. Noh and J. c. Hwang, "Second-order perturbations of the Friedmann world model," Phys. Rev. D **69** (2004), 104011

- [19] C. Carbone and S. Matarrese, “A Unified treatment of cosmological perturbations from super-horizon to small scales,” *Phys. Rev. D* **71** (2005), 043508 [[astro-ph/astro-ph/0407611](#)].
- [20] K. Nakamura, “Second-order gauge invariant cosmological perturbation theory: Einstein equations in terms of gauge invariant variables,” *Prog. Theor. Phys.* **117** (2007), 17-74 [[gr-qc/gr-qc/0605108](#)].
- [21] N. Aghanim *et al.* [Planck], “Planck 2018 results. VI. Cosmological parameters,” *Astron. Astrophys.* **641** (2020), A6 [[astro-ph.CO/1807.06209](#)].
- [22] R. Allahverdi, M. A. Amin, A. Berlin, N. Bernal, C. T. Byrnes, M. Sten Delos, A. L. Erickcek, M. Escudero, D. G. Figueroa and K. Freese, *et al.* “The First Three Seconds: a Review of Possible Expansion Histories of the Early Universe,” [[astro-ph.CO/2006.16182](#)].
- [23] S. Mollerach, D. Harari and S. Matarrese, “CMB polarization from secondary vector and tensor modes,” *Phys. Rev. D* **69** (2004), 063002 [[astro-ph/astro-ph/0310711](#)].
- [24] K. N. Ananda, C. Clarkson and D. Wands, “The Cosmological gravitational wave background from primordial density perturbations,” *Phys. Rev. D* **75** (2007), 123518 [[gr-qc/gr-qc/0612013](#)].
- [25] D. Baumann, P. J. Steinhardt, K. Takahashi and K. Ichiki, “Gravitational Wave Spectrum Induced by Primordial Scalar Perturbations,” *Phys. Rev. D* **76** (2007), 084019 [[hep-th/hep-th/0703290](#)].
- [26] V. De Luca, V. Desjacques, G. Franciolini and A. Riotto, “Gravitational Waves from Peaks,” *JCAP* **09** (2019), 059 [[astro-ph.CO/1905.13459](#)].
- [27] G. Domènech, “Induced gravitational waves in a general cosmological background,” *Int. J. Mod. Phys. D* **29** (2020) no.03, 2050028 [[gr-qc/1912.05583](#)].
- [28] G. Domènech, S. Pi and M. Sasaki, *JCAP* **08** (2020), 017 doi:10.1088/1475-7516/2020/08/017 [[arXiv:2005.12314](#) [gr-qc]].
- [29] I. Dalianis and K. Kritos, “Exploring the Spectral Shape of Gravitational Waves Induced by Primordial Scalar Perturbations and Connection with the Primordial Black Hole Scenarios,” [[astro-ph.CO/2007.07915](#)].
- [30] H. Assadullahi and D. Wands, “Gravitational waves from an early matter era,” *Phys. Rev. D* **79** (2009), 083511 [[astro-ph.CO/0901.0989](#)].
- [31] K. Inomata, K. Kohri, T. Nakama and T. Terada, “Enhancement of Gravitational Waves Induced by Scalar Perturbations due to a Sudden Transition from an Early Matter Era to the Radiation Era,” *Phys. Rev. D* **100** (2019) no.4, 043532 [[astro-ph.CO/1904.12879](#)].
- [32] K. Inomata, K. Kohri, T. Nakama and T. Terada, “Gravitational Waves Induced by Scalar Perturbations during a Gradual Transition from an Early Matter Era to the Radiation Era,” *JCAP* **10** (2019), 071 [[astro-ph.CO/1904.12878](#)].
- [33] J. C. Hwang, D. Jeong and H. Noh, “Gauge dependence of gravitational waves generated from scalar perturbations,” *Astrophys. J.* **842** (2017) no.1, 46 [[astro-ph.CO/1704.03500](#)].
- [34] J. O. Gong, “Analytic integral solutions for induced gravitational waves,” [[gr-qc/1909.12708](#)].
- [35] K. Tomikawa and T. Kobayashi, “Gauge dependence of gravitational waves generated at second order from scalar perturbations,” *Phys. Rev. D* **101** (2020) no.8, 083529 [[gr-qc/1910.01880](#)].
- [36] V. De Luca, G. Franciolini, A. Kehagias and A. Riotto, “On the Gauge Invariance of Cosmological Gravitational Waves,” *JCAP* **03** (2020), 014 doi:10.1088/1475-7516/2020/03/014 [[arXiv:1911.09689](#) [gr-qc]].
- [37] K. Inomata and T. Terada, “Gauge Independence of Induced Gravitational Waves,” *Phys. Rev. D* **101** (2020) no.2, 023523 [[arXiv:1912.00785](#) [gr-qc]].
- [38] Z. Chang, S. Wang and Q. H. Zhu, “Gauge Invariant Second Order Gravitational Waves,” [[gr-qc/2009.11994](#)].

- [39] Z. Chang, S. Wang and Q. H. Zhu, “On the Gauge Invariance of Scalar Induced Gravitational Waves: Gauge Fixings Considered,” [[gr-qc/2010.01487](#)].
- [40] G. Domènech and M. Sasaki, “Approximate gauge independence of the induced gravitational wave spectrum,” *Phys. Rev. D* **103** (2021) no.6, 063531 [[gr-qc/2012.14016](#)].
- [41] Y. B. Zeldovich, “Gravitational instability: An Approximate theory for large density perturbations,” *Astron. Astrophys.* **5** (1970), 84-89
- [42] F. Bernardeau, S. Colombi, E. Gaztanaga and R. Scoccimarro, “Large scale structure of the universe and cosmological perturbation theory,” *Phys. Rept.* **367** (2002), 1-248 [[0112551/astro-ph](#)]
- [43] K. S. Thorne, “NONSPHERICAL GRAVITATIONAL COLLAPSE: A SHORT REVIEW,”
- [44] C. W. Misner, K. S. Thorne and J. A. Wheeler, “Gravitation”
- [45] D. Lynden-Bell, “Statistical mechanics of violent relaxation in stellar systems,” *Mon. Not. Roy. Astron. Soc.* **136** (1967), 101-121
- [46] K. Jedamzik, M. Lemoine and J. Martin, “Generation of gravitational waves during early structure formation between cosmic inflation and reheating,” *JCAP* **04** (2010), 021 [[astro-ph.CO/1002.3278](#)].
- [47] T. Nakama, “Stochastic gravitational waves associated with primordial black holes formed during an early matter era,” *Phys. Rev. D* **101** (2020) no.6, 063519
- [48] I. Dalianis, A. Kehagias and G. Tringas, “Primordial black holes from α -attractors,” *JCAP* **01** (2019), 037 [[astro-ph.CO/1805.09483](#)].
- [49] I. Dalianis and G. Tringas, “Primordial black hole remnants as dark matter produced in thermal, matter, and runaway-quintessence postinflationary scenarios,” *Phys. Rev. D* **100** (2019) no.8, 083512 [[astro-ph.CO/1905.01741](#)].
- [50] G. Ballesteros, J. Rey and F. Rompineve, “Detuning primordial black hole dark matter with early matter domination and axion monodromy,” *JCAP* **06** (2020), 014 [[astro-ph.CO/1912.01638](#)].
- [51] T. Harada, C. M. Yoo, K. Kohri, K. i. Nakao and S. Jhingan, “Primordial black hole formation in the matter-dominated phase of the Universe,” *Astrophys. J.* **833** (2016) no.1, 61 [[astro-ph.CO/1609.01588](#)].
- [52] V. Mukhanov, “Physical Foundations of Cosmology”
- [53] A.G. Doroshkevich, 1970 *Astrophysica* 6 30
- [54] P.J.E. Peebles, 1970 *Astrophysica* 6 30 “Large Scale Structure of the Universe”, (Princeton Univ Press, Princeton, 1980)
- [55] J. c. Hwang, H. Noh and J. O. Gong, “Second order solutions of cosmological perturbation in the matter dominated era,” *Astrophys. J.* **752** (2012), 50 [[astro-ph.CO/1204.3345](#)].
- [56] M. Y. Khlopov and A. G. Polnarev, “Primordial Black Holes As A Cosmological Test Of Grand Unification,” *Phys. Lett.* **97B** (1980) 383.
- [57] A. G. Polnarev and M. Y. Khlopov, “Cosmology, Primordial Black Holes, And Supermassive Particles,” *Sov. Phys. Usp.* **28** (1985) 213 [*Usp. Fiz. Nauk* **145** (1985) 369].
- [58] T. Harada, C. M. Yoo, K. Kohri and K. I. Nakao, “Spins of primordial black holes formed in the matter-dominated phase of the Universe,” *Phys. Rev. D* **96** (2017) no.8, 083517 [erratum: *Phys. Rev. D* **99** (2019) no.6, 069904] [[gr-qc/1707.03595](#)].
- [59] I. Hawke and J. M. Stewart, “The dynamics of primordial black hole formation,” *Class. Quant. Grav.* **19** (2002), 3687-3707
- [60] B. J. Carr, K. Kohri, Y. Sendouda and J. Yokoyama, “New cosmological constraints on primordial black holes,” *Phys. Rev. D* **81** (2010), 104019 [[astro-ph.CO/0912.5297](#)].
- [61] D. N. Page and S. W. Hawking, “Gamma rays from primordial black holes,” *Astrophys. J.* **206** (1976), 1-7

- [62] J. H. MacGibbon and B. J. Carr, “Cosmic rays from primordial black holes,” *Astrophys. J.* **371** (1991), 447-469
- [63] B. J. Carr and J. H. MacGibbon, “Cosmic rays from primordial black holes and constraints on the early universe,” *Phys. Rept.* **307** (1998), 141-154
- [64] A. Barrau, G. Boudoul and L. Derome, “An improved gamma-ray limit on the density of pbhs,” [[astro-ph/astro-ph/0304528](#)].
- [65] B. J. Carr, K. Kohri, Y. Sendouda and J. Yokoyama, “Constraints on primordial black holes from the Galactic gamma-ray background,” *Phys. Rev. D* **94** (2016) no.4, 044029 [[astro-ph.CO/1604.05349](#)].
- [66] B. Dasgupta, R. Laha and A. Ray, “Neutrino and positron constraints on spinning primordial black hole dark matter,” *Phys. Rev. Lett.* **125** (2020) no.10, 101101 [[hep-ph/1912.01014](#)].
- [67] A. Barnacka, J. F. Glicenstein and R. Moderski, “New constraints on primordial black holes abundance from femtolensing of gamma-ray bursts,” *Phys. Rev. D* **86** (2012), 043001 [[astro-ph.CO/1204.2056](#)].
- [68] P. Tisserand *et al.* [EROS-2], “Limits on the Macho Content of the Galactic Halo from the EROS-2 Survey of the Magellanic Clouds,” *Astron. Astrophys.* **469** (2007), 387-404 [[astro-ph/astro-ph/0607207](#)].
- [69] H. Niikura, M. Takada, N. Yasuda, R. H. Lupton, T. Sumi, S. More, T. Kurita, S. Sugiyama, A. More and M. Oguri, *et al.* “Microlensing constraints on primordial black holes with Subaru/HSC Andromeda observations,” *Nature Astron.* **3** (2019) no.6, 524-534 [[astro-ph.CO/1701.02151](#)].
- [70] M. Ricotti, J. P. Ostriker and K. J. Mack, “Effect of Primordial Black Holes on the Cosmic Microwave Background and Cosmological Parameter Estimates,” *Astrophys. J.* **680** (2008), 829 [[astro-ph/0709.0524](#)].
- [71] B. Carr, F. Kuhnel and M. Sandstad, “Primordial Black Holes as Dark Matter,” *Phys. Rev. D* **94** (2016) no.8, 083504 [[astro-ph.CO/1607.06077](#)].
- [72] S. Clesse and J. García-Bellido, “The clustering of massive Primordial Black Holes as Dark Matter: measuring their mass distribution with Advanced LIGO,” *Phys. Dark Univ.* **15** (2017), 142-147 [[astro-ph.CO/1603.05234](#)].
- [73] S. Bird, I. Cholis, J. B. Muñoz, Y. Ali-Haïmoud, M. Kamionkowski, E. D. Kovetz, A. Racanelli and A. G. Riess, “Did LIGO detect dark matter?,” *Phys. Rev. Lett.* **116** (2016) no.20, 201301 [[astro-ph.CO/1603.00464](#)].
- [74] V. Poulin, P. D. Serpico, F. Calore, S. Clesse and K. Kohri, “CMB bounds on disk-accreting massive primordial black holes,” *Phys. Rev. D* **96** (2017) no.8, 083524 [[astro-ph.CO/1707.04206](#)].
- [75] P. D. Serpico, V. Poulin, D. Inman and K. Kohri, “Cosmic microwave background bounds on primordial black holes including dark matter halo accretion,” *Phys. Rev. Res.* **2** (2020) no.2, 023204 [[astro-ph.CO/2002.10771](#)].
- [76] D. Gaggero, G. Bertone, F. Calore, R. M. T. Connors, M. Lovell, S. Markoff and E. Storm, “Searching for Primordial Black Holes in the radio and X-ray sky,” *Phys. Rev. Lett.* **118** (2017) no.24, 241101 [[astro-ph.HE/1612.00457](#)].
- [77] B. Carr, K. Kohri, Y. Sendouda and J. Yokoyama, “Constraints on Primordial Black Holes,” [[astro-ph.CO/2002.12778](#)].
- [78] D. P. Quinn, M. I. Wilkinson, M. J. Irwin, J. Marshall, A. Koch and V. Belokurov, “On the Reported Death of the MACHO Era,” *Mon. Not. Roy. Astron. Soc.* **396** (2009), 11 [[astro-ph.GA/0903.1644](#)].
- [79] T. D. Brandt, “Constraints on MACHO Dark Matter from Compact Stellar Systems in Ultra-Faint Dwarf Galaxies,” *Astrophys. J. Lett.* **824** (2016) no.2, L31 [[astro-ph.GA/1605.03665](#)].

- [80] B. P. Abbott *et al.* [LIGO Scientific and Virgo], “Search for Substellar-Mass Ultracompact Binaries in Advanced LIGO’s First Observing Run,” *Phys. Rev. Lett.* **121** (2018) no.23, 231103 [[astro-ph.CO/1808.04771](#)].
- [81] G. Hütsi, M. Raidal, V. Vaskonen and H. Veermäe, “Two populations of LIGO-Virgo black holes,” [[astro-ph.CO/2012.02786](#)].
- [82] M. Raidal, V. Vaskonen and H. Veermäe, “Gravitational Waves from Primordial Black Hole Mergers,” *JCAP* **09** (2017), 037 [[astro-ph.CO/1707.01480](#)].
- [83] K. Jedamzik, “Consistency of Primordial Black Hole Dark Matter with LIGO/Virgo Merger Rates,” *Phys. Rev. Lett.* **126** (2021) no.5, 051302 [[astro-ph.CO/2007.03565](#)].
- [84] Z. Arzoumanian *et al.* [NANOGrav], “The NANOGrav 12.5 yr Data Set: Search for an Isotropic Stochastic Gravitational-wave Background,” *Astrophys. J. Lett.* **905** (2020) no.2, L34 [[astro-ph.HE/2009.04496](#)].
- [85] S. E. Thorsett and R. J. Dewey, “Pulsar timing limits on very low frequency stochastic gravitational radiation,” *Phys. Rev. D* **53** (1996), 3468-3471
- [86] R. Saito and J. Yokoyama, “Gravitational wave background as a probe of the primordial black hole abundance,” *Phys. Rev. Lett.* **102** (2009), 161101 [erratum: *Phys. Rev. Lett.* **107** (2011), 069901] [[astro-ph/0812.4339](#)].
- [87] E. Bugaev and P. Klimai, “Constraints on the induced gravitational wave background from primordial black holes,” *Phys. Rev. D* **83** (2011), 083521 [[astro-ph.CO/1012.4697](#)].
- [88] J. Crowder and N. J. Cornish, “Beyond LISA: Exploring future gravitational wave missions,” *Phys. Rev. D* **72** (2005), 083005 [[gr-qc/0506015](#)].
- [89] R. Abbott *et al.* [LIGO Scientific and Virgo], “GW190814: Gravitational Waves from the Coalescence of a 23 Solar Mass Black Hole with a 2.6 Solar Mass Compact Object,” *Astrophys. J. Lett.* **896** (2020) no.2, L44 [[astro-ph.HE/2006.12611](#)].
- [90] G. Janssen, G. Hobbs, M. McLaughlin, C. Bassa, A. T. Deller, M. Kramer, K. Lee, C. Mingarelli, P. Rosado and S. Sanidas, *et al.* “Gravitational wave astronomy with the SKA,” *PoS AASKA14* (2015), 037 [[astro-ph.IM/1501.00127](#)].
- [91] R. Maartens *et al.* [SKA Cosmology SWG], “Overview of Cosmology with the SKA,” *PoS AASKA14* (2015), 016 [[astro-ph.CO/1501.04076](#)].
- [92] J. Lu, K. Lee and R. Xu, “Advancing Pulsar Science with the FAST,” *Sci. China Phys. Mech. Astron.* **63** (2020) no.2, 229531 [[astro-ph.HE/1909.03707](#)].
- [93] N. Bhaumik and R. K. Jain, “Stochastic induced gravitational waves and lowest mass limit of primordial black holes with the effects of reheating,” [[astro-ph.CO/2009.10424](#)].
- [94] J. D. Barrow, E. J. Copeland and A. R. Liddle, “The Cosmology of black hole relics,” *Phys. Rev. D* **46** (1992), 645-657
- [95] B. J. Carr, J. H. Gilbert and J. E. Lidsey, “Black hole relics and inflation: Limits on blue perturbation spectra,” *Phys. Rev. D* **50** (1994), 4853-4867 [[astro-ph/astro-ph/9405027](#)].